Dielectric screening and band-structure effects in low-energy photoemission

E. E. Krasovskii,[1,2,3] V. M. Silkin,[1,2,3] V. U. Nazarov,[4] P. M. Echenique,[1,2,5] and E. V. Chulkov[1,2,5]
[1]*Departamento de Física de Materiales, Facultad de Ciencias Químicas, Universidad del Pais Vasco/Euskal Herriko Unibertsitatea, Apdo. 1072, San Sebastián/Donostia, 20080 Basque Country, Spain*
[2]*Donostia International Physics Center (DIPC), Paseo Manuel de Lardizabal 4, San Sebastián/Donostia, 20018 Basque Country, Spain*
[3]*IKERBASQUE, Basque Foundation for Science, 48011 Bilbao, Spain*
[4]*Research Center for Applied Sciences, Academia Sinica, Taipei 115, Taiwan*
[5]*Centro de Física de Materiales (CFM), Materials Physics Center (MPC), Centro Mixto CSIC–UPV/EHU, Edificio Korta, Avenida de Tolosa 72, 20018 San Sebastián, Spain*
(Received 21 July 2010; published 3 September 2010)

Nonlocal response of the surface to the incident light is included into an *ab initio* one-step photoemission theory. Surface-state normal emission spectra from Be(0001) and Al(100) are calculated by a full-potential scattering method and are found to agree well with the experiment in a wide energy range. The total exciting field is obtained within the random-phase approximation for jellium as well as for one-dimensional crystal models of the two surfaces. Material dependence of the multipole plasmon mode and strong effect of band structure on the photoyield is discussed.

DOI: 10.1103/PhysRevB.82.125102 PACS number(s): 79.60.−i, 73.20.Mf

I. INTRODUCTION

Over recent years interest has grown in photoemission at low photon energies: the ability to reach a higher bulk sensitivity of angle-resolved photoemission spectroscopy (ARPES) at lower kinetic energies has given rise to the development of new laser[1] and synchrotron-based[2] light sources. A related issue of fundamental and technological interest is the design of laser-driven photocathodes of high quantum efficiency for free-electron lasers.[3] At the photon energies of a few electron volts the dielectric response of the crystal becomes important. In particular, in metals, below the plasmon energy the microscopic fields generated at the surface by *p*-polarized light greatly enhance the emission intensity.[4] Another important aspect of the low kinetic-energy regime is that the photocurrent strongly depends on the elastic scattering in the bulk and at the surface (low-energy electron diffraction, LEED). This calls for an *ab initio* photoemission theory that incorporates a spatially variable exciting electric field.

Experimentally, the enhancement of total photoyield below the bulk plasma frequency ω_p is well studied for simple metals.[5] Especially informative is the constant initial state (CIS) mode of ARPES because the photoelectron initial and final states are well defined. Low-energy CIS spectra were reported for Al(100) in Ref. 6 and then for Be(0001) in Ref. 7 and Al(111) in Ref. 8.

Qualitatively, the emission enhancement is well understood as due to the excitation of a multipole surface plasmon,[9] which had been predicted to appear for a sufficiently smoothly decaying electronic density at the surface.[10] The multipole mode is a result of the nonlocal dielectric response at the surface. It was obtained by Feibelman[11] in the random-phase approximation (RPA) for the response function in a jellium model. The local-field enhancement and the power absorption at the surface are presently well understood,[4] however, the question whether the absolute values of the predicted local fields are realistic has never been raised. In metals with high electronic density, such as Al and Be, the multipole plasmon is only weakly manifested in electron-energy-loss spectra[12] because it is blurred by a strong surface monopole plasmon. Thus, photoemission experiment is the only way to answer the question. For reliable conclusions, the spectrum must include also the high-energy region, where the exciting field is spatially constant, and which may serve as the reference to measure the intensity of local fields. Till now only a few theoretical studies considered the effect of induced fields on photocurrent, and they all were restricted to low energies. The jellium model[11] described rather well the shape of the measured Fermi-level CIS spectrum of Al(100),[6] but further attempts to reproduce the surface-state spectrum of Al(100) within simplified models for the band structure[13,14] gave only a qualitative agreement with the experiment.

In the present study we go beyond the qualitative understanding of photocurrent in terms of power absorption and apply a microscopic theory to the two available experiments on surface-state emission: to the well-studied case of Al(100) and to Be(0001), which has not been theoretically addressed. Our aim is to elucidate the relation between the spatial structure of the electric field and the photoemission intensity and to reveal the role of the actual band structure. This role is threefold: (i) the nonfree-electron character of the photoemission initial and final states, (ii) the effect of optical absorption due to interband transitions on the *classical* Fresnel field, and (iii) the effect of crystallinity on the nonlocal dielectric response. In the present theory the first aspect is fully taken into account: the spatially varying exciting field is included into a one-step theory of photoemission[15,16] based on an all-electron self-consistent full potential both in the bulk and at the surface. The classical field in vacuum E^{vac} is derived from the Fresnel equations using experimental dielectric function (DF) from Ref. 17. The nonlocal response is treated approximately: apart from the well-studied jellium model we shall consider a more general case of one-dimensional (1D) crystallinity, which introduces the damping due to electron-hole excitations, albeit underestimated, and eliminates the uncertainty of the jellium model in locating

the edge of the positive background relative to the crystal surface.

II. SURFACE DIELECTRIC RESPONSE

For a system inhomogeneous only in the surface-normal direction z, the z component of the electric field is the solution of the 1D integral equation

$$\int \epsilon^{zz}(z,z';\omega)E_z(z';\omega)dz' = D_z = E_z^{\mathrm{vac}}. \tag{1}$$

The classical field E_z^{vac} is fixed by the experimental DF ϵ_{mac} and the approximate microscopic theory is used to derive the spatially varying total field. To obtain the total exciting field we follow the approach by Samuelsen and Schattke,[18] which reduces the calculation of the response to the transverse field to the response to a scalar field, with the external scalar field taken as an evanescent wave

$$\phi^{\mathrm{ext}}(\mathbf{r}) = -(2\pi/q)\exp(i\mathbf{q}_{\parallel}\mathbf{r}_{\parallel} + qz)$$

with $q=q_{\parallel}$. The limit $q\to 0$ is ensured by the numerical convergence of the results for $2\pi/q$ much larger than the lattice constant.

In the present work the self-consistent RPA response function is calculated in a finite-thickness slab geometry[19] (60 atomic layers for both surfaces) for the laterally averaged model potential,[20] which is constructed so as to give the correct parameters of the gap at $\bar{\Gamma}$ and the location of the surface state. It is straightforward to generalize this scheme to a true three-dimensional crystal potential, however, this exceeds our present computer capabilities.

The response of the electronic system to the external scalar field ϕ^{ext} is determined by the equation

$$\int dz'\,\chi_0(z,z';q,\omega)\phi^{\mathrm{tot}}(z';q,\omega) = \int dz'\,\chi(z,z';q,\omega)\phi^{\mathrm{ext}}(z';q,\omega), \tag{2}$$

where ϕ^{tot} is the total self-consistent field and the functions χ_0 and χ are the two-dimensional (2D) Fourier transforms of the noninteracting and interacting density-response functions, respectively. The noninteracting response function is derived from the single-particle eigenfunctions ψ_n, which in the geometry of thick repeated slabs are standing waves in the surface perpendicular direction and are independent of the surface parallel Bloch vector $\mathbf{k}_{\parallel}$

$$\chi_0(z,z';q,\omega) = 2\sum_{n,m}\psi_n(z)\psi_m^*(z)\psi_n^*(z')\psi_m(z') \times \sum_{\mathbf{k}_{\parallel}}\frac{f_{\mathbf{k}_{\parallel},n} - f_{\mathbf{k}_{\parallel}+\mathbf{q},m}}{E_{\mathbf{k}_{\parallel},n} - E_{\mathbf{k}_{\parallel}+\mathbf{q},m} + \omega + i\eta}. \tag{3}$$

Here the sum over n and m comprises both occupied and unoccupied states and $f_{\mathbf{k}_{\parallel},n}=\Theta(E_{\mathrm{F}}-E_{\mathbf{k}_{\parallel},n})$ are the Fermi occupation factors.

Within the RPA, the interacting response function χ is the solution of the integral equation

$$\chi(z,z';q,\omega) = \chi_0(z,z';q,\omega) + \int dz_1\int dz_2\chi_0(z,z_1;q,\omega) \times v(z_1,z_2;q)\chi(z_2,z';q,\omega), \tag{4}$$

where $v(z_1,z_2;q)$ is the 2D Fourier transform of the bare Coulomb interaction. In the present approach the integral equation reduces to a linear algebra matrix equation (more details of the calculations are given in Ref. 19).

The solution of Eq. (1) $E_z(z';\omega)$ is obtained from the solution ϕ^{tot} of Eq. (2) as its gradient $-d\phi^{\mathrm{tot}}/dz$ scaled so as to equal the z projection of the electric field of the electromagnetic wave in vacuum E_z^{vac}. In the present approach the latter is determined from the classical Fresnel equations.

III. ONE-STEP PHOTOEMISSION THEORY

In the one-step theory[21] the photocurrent is given by the transition probability from the initial state $|\mathrm{i}\rangle$ of energy E to the time-reversed LEED state $|\mathrm{f}\rangle$ of energy $E+\hbar\omega$

$$J(\omega) \sim \sqrt{K}|\langle \mathrm{f}|\Delta\hat{H}|\mathrm{i}\rangle|^2, \tag{5}$$

where K is the final kinetic energy. The surface state $|\mathrm{i}\rangle$ is a discrete eigenstate of the semi-infinite crystal and the LEED state is a scattering solution for a plane wave incident from vacuum. A self-consistent (in the local-density approximation) crystal potential is constructed with the full-potential linear augmented plane-wave (APW) method.[22] The potential at the surface is calculated in a repeated slab geometry (ten layers for Be and 17 layers for Al with vacuum intervals between the slabs). The surface is embedded between the bulk and the vacuum half spaces, and the wave functions of surface and LEED states are calculated with the APW-based scattering technique described in Ref. 15; the specific application to photoemission from surface states was presented in Ref. 16.

To calculate the matrix elements in Eq. (5), the all-electron wave functions are expanded in plane waves using the gouging technique introduced in Ref. 22: each atom is surrounded by a small sphere (0.5 a.u. radius), within which the wave function is damped to reduce its oscillations. The resulting pseudowave function has a rapidly convergent plane-wave expansion, which facilitates the calculation, and only a small contribution to the matrix element from the close vicinity of the nuclei is lost. The high quality of this approximation for the calculation of momentum matrix elements was demonstrated in Ref. 23. When the spatially varying field is included the integration over z is performed in real space limited to the depth of 50 a.u. inside the crystal, which introduces a negligible error.

The inelastic scattering of the outgoing electron is described by the imaginary potential $-iV_{\mathrm{i}}$ added to the Hamiltonian in the crystal half space. This is the only unknown parameter of the theory, however, according to previous experience,[24,25] it is not strongly material dependent and has a common behavior: V_{i} is close to zero at the Fermi energy, sharply increases at ω_{p} and then steadily grows with energy. Assuming this shape, we deduced the functions $V_{\mathrm{i}}(E)$ from previous results for Al(100) (Ref. 25) with an expected un-

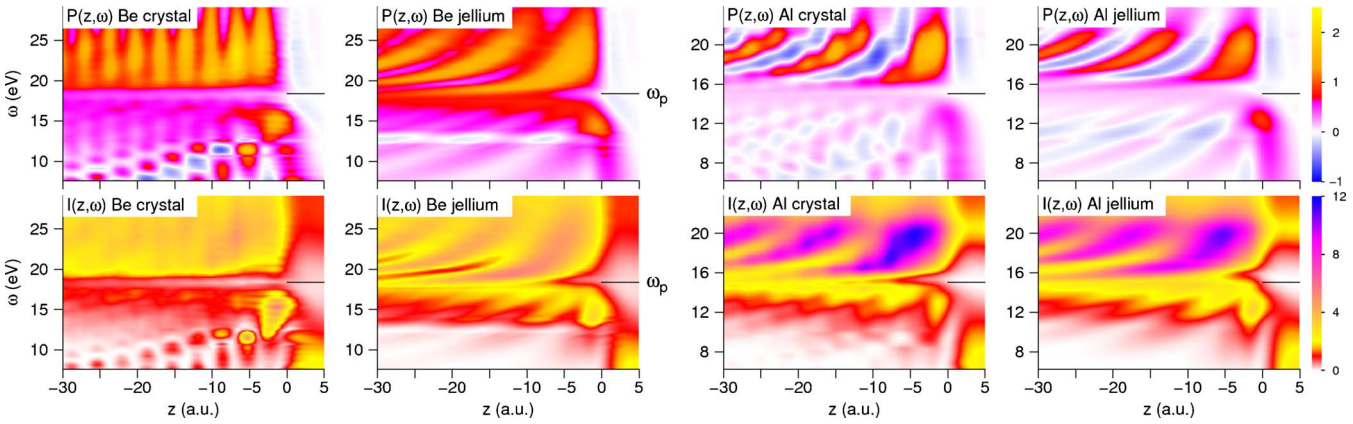

FIG. 1. (Color online) Power absorption density $P(z,\omega)=(\omega/4\pi)\mathrm{Im}[D_z E_z^*(z,\omega)]$ (upper row) and intensity $I(z,\omega)=|E_z(z,\omega)|^2$ (lower row) for Be(0001) (first and second columns) and Al(100) (third and fourth columns). Calculation are for $q=0.02$ a.u.$^{-1}$.

certainty of ± 0.5 eV. The $V_i(E)$ curve for Be(0001) is shown in the inset of Fig. 3 and estimated intensity uncertainty is shown in Figs. 2(c), 2(d), and 3(b) by shading.

IV. RESULTS AND DISCUSSION

In the jellium case, light is absorbed only at the surface, and the absorbed power is proportional to the imaginary part of the centroid of the induced density $d_\perp(\omega)$.[4] In a crystal, owing to the bulk local fields, the induced microscopic dipole moment extends to macroscopic distances, and surface and bulk absorption cannot be unambiguously separated. The surface absorption is, however, clearly seen in the energy-depth distribution $P(z,\omega)$ of the absorbed power: the results for the 1D crystal and jellium models of Al(100) and Be(0001) for p-polarized light incident at 45° are shown in Fig. 1 along with field intensity $I(z,\omega)$, which is the relevant quantity for photoemission. Above ω_p bulk plasmons are excited, the momentum being provided by the surface: the plasmon wave vector increasing with energy is clearly seen for jellium models and for crystalline Al, but in Be it is blurred by the more strong crystal fields. Below ω_p surface absorption peaks at the multipole plasmon energy $\omega_m \sim 0.8\omega_p$ in all cases, in perfect agreement with the earlier jellium theory.[4] For a more detailed comparison, in Fig. 2 we show vertical cross sections at the surface of the maps of Fig. 1.

The effect of optical absorption $\mathrm{Im}\,\epsilon_{mac}$ on intensity $I(z,\omega)$ is negligible below ω_p, but around the classical resonance $\omega_c=\omega_p\sqrt{2}$, where reflected and incident field are in phase, it is very strong, e.g., in Be it reduces the field intensity by a factor of 4. This was found by replacing the experimental DF with the Drude expression.

In the jellium model, the field intensities below ω_p are very close for Al and Be, see $I_s(\omega)$ curves in Figs. 2(a) and 2(b), as expected from their close bulk electronic densities. However, the inclusion of the 1D crystallinity introduces dramatic differences: the multipole peak becomes much higher and sharper in Be(0001) than in Al(100). To see how these features are manifested in photoemission we shall include the calculated total field into the perturbation operator $\Delta\hat{H}=\mathbf{A}(\mathbf{r},\omega)\cdot\hat{\mathbf{p}}+\hat{\mathbf{p}}\cdot\mathbf{A}(\mathbf{r},\omega)$ of Eq. (5)

The calculated photon-energy dependence of the normal emission intensity (J_{scr} for the screened field and J_{wos} without screening) from the surface states on Al(100) and on Be(0001) is compared to the measurements in Figs. 2(c) and 2(d). The spectra with screened exciting field are in good agreement with the experiment regarding the energy location and the shape of the two maxima due to dielectric response: the multipole plasmon at ω_m and the classical resonance at ω_c. The $J_{wos}(\omega)$ curve [with $E_z(z;\omega)=\mathrm{const}$] shows distinct

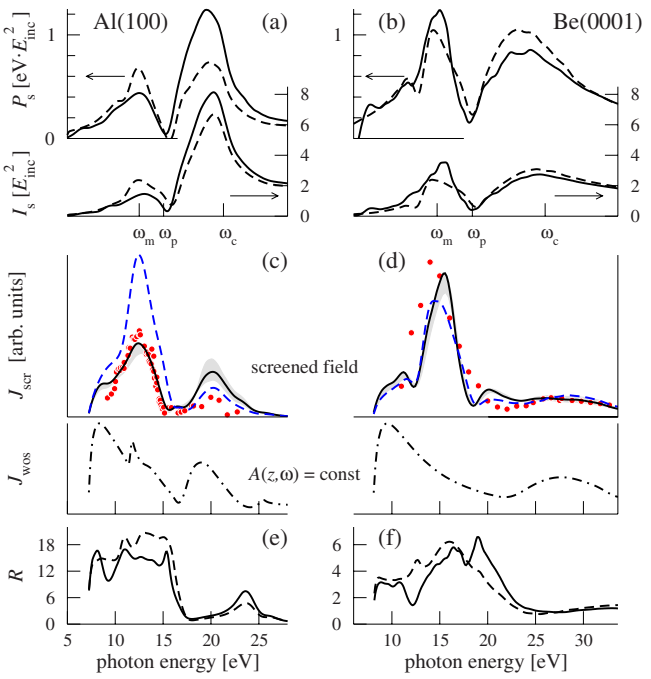

FIG. 2. (Color online) Effect of screening in Al(100) (left) and Be(0001) (right). [(a) and (b)] Power absorption density $P_s(\omega)$ and field intensity $I_s(\omega)$ at the surface are the average of the $P(z,\omega)$ and $I(z,\omega)$ maps in Fig. 1 over a range from $z=-4$ to 1 a.u. In all graphs solid lines are for 1D crystal and dashed for jellium. [(c) and (d)] Surface-state intensity with (solid and dashed lines) and without screening (dotted-dashed). Shading shows the estimated error due to the uncertainty in optical potential V_i of ± 0.5 eV. Circles are the measurements for Al(100) (Ref. 6) and for Be(0001) (Ref. 7). [(e) and (f)] Reactivity $R=J_{scr}/[J_{wos}I_s]$.

structures due to quasidirect transitions, in contrast to its previous interpretation as pure surface photoeffect.[11,13] The band-structure effects influence also the emission by the screened field, which can be expressed by the reactivity $R(\omega)=J_{scr}(\omega)/[J_{wos}(\omega)I_s(\omega)]$, see Figs. 2(e) and 2(f). The dimensionless normalization factor $I_s(\omega)$ (average intensity at the surface in units of incident intensity, see the caption of Fig. 2) is introduced to eliminate the dependence on the amplitude of the total field, which strongly varies with ω. Thus, $R(\omega)$ is sensitive to the spatial structure of the exciting field and can be thought of as its form factor since for a spatially uniform field it is unity. The normalization by $I_s(\omega)$ is somewhat arbitrary, but the similar overall shape of the curves for jellium and for 1D crystal models suggests that this is a reasonable choice. The $R(\omega)$ curves reveal the difference between the two metals: Al turns out three times more reactive to the multipole mode than Be. Of course, the values depend on the initial state, and they would be different for the total photoyield, but this example gives an estimate of how strong its material dependence may be.

Finally, we prove that our theory gives realistic values for the strength of the exciting field and for the enhancement of photoyield. Figure 3 compares our results for the 1D crystal to the experiment on Be(0001).[7] The region well above ω_p, where the dielectric response is negligible, provides the required reference. The spectral shape is well described over the whole range, in particular, the structures B–E that manifest the strongly nonfree-electron character of the final states: Fig. 3(a) relates the maxima B–E to the complex band structure of the LEED states in the $A\Gamma A$ interval of the bulk Brillouin zone. The intensity is distributed over several conducting branches (i.e., partial waves that effect the escape of the photoelectron), and the observed spectrum results from a superposition of transition amplitudes to different Bloch waves.

The theory rather accurately describes the intensity variation by 2 orders of magnitude in the interval 10–50 eV, although it does not account for the further decrease in intensity at higher energies. Assuming that the higher intensities are experimentally more reliable, in Fig. 3 we adjusted the curves so as to match over the interval 25–45 eV. The good agreement in the intensity of the multipole plasmon peak suggests that the present model for the dielectric response is adequate for real surfaces. Still, both in Be and in Al the theory underestimates the intensity of the multipole plasmon peak relative to the classical enhancement at ω_c. In the experiment, an additional enhancement of photoemission may be caused by the contribution from the radiative decay of the monopole plasmon at $\omega_p/\sqrt{2}$, which may couple to light due to the surface roughness.

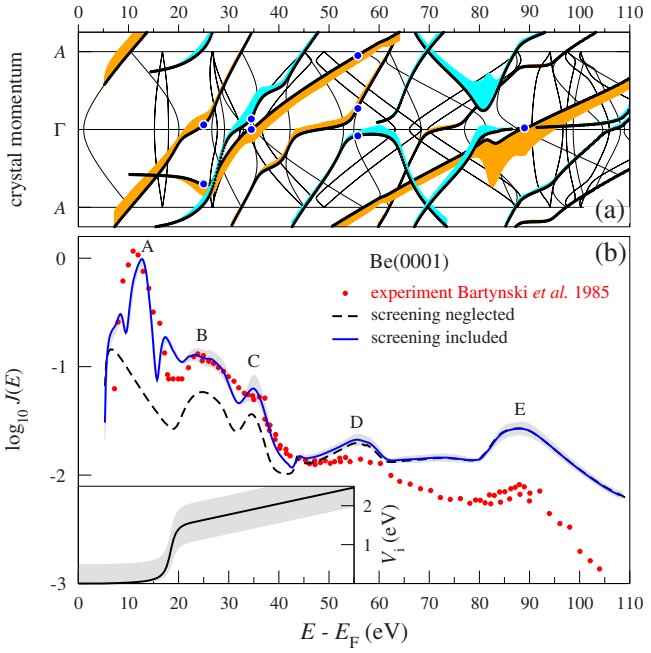

FIG. 3. (Color online) (a) Complex band structure of Be(0001) at $\bar{\Gamma}$: thick lines show Bloch waves that contribute to LEED states. Vertical extent of shading is proportional to the modulus (not squared) of the contribution to the matrix element from the individual partial wave. Circles indicate $k_\perp$ vectors of the Bloch waves at the maxima B–E. Thin lines are the bulk band structure in the $A\Gamma A$ interval. (b) Experimental (Ref. 7) semilogarithmic intensity profile $\log_{10} J(\omega)$ (circles) of the $\bar{\Gamma}$ surface state emission compared to the theory with (solid line) and without screening (dashed). Inset: optical potential $V_i(E)$. Shading shows the estimated uncertainty of V_i and in graph (b) the related intensity uncertainty.

V. SUMMARY

To summarize, we have incorporated the spatial structure of the exciting field into an *ab initio* one-step theory and have presented the evidence that the induced field obtained within the nonlocal RPA is very realistic. We have compared the jellium and the 1D crystal models for the dielectric response and have found the 1D crystallinity to have only a minor effect on the energy location of the multipole plasmon. However, the amplitude of the exciting field is considerably affected, which means that it may be rather different in materials with close average electronic densities.

In the simple metals Al and Be the final states are proved to be far from free-electronlike, and the emission both at low and at high energies is not a pure surface photoeffect. This causes the material dependence of the multipole plasmon enhancement of photoemission, which, for the surface-state emission, in Al(100) is three times higher than in Be(0001). Thus, both the effect of crystal structure on the electric field at the surface and on the photoemission final states should be taken into account in order to understand low-energy spectra, and the present approach provides a practicable scheme to include both effects.

ACKNOWLEDGMENTS

The authors gratefully acknowledge fruitful discussions with W. Schattke, A. Liebsch, and V. Strocov. The authors acknowledge partial support from the University of the Basque Country (Grant No. GIC07IT36607) and the Spanish Ministerio de Ciencia y Tecnología (Grant No. FIS2007-66711-C02-01).

[1] J. D. Koralek, J. F. Douglas, N. C. Plumb, Z. Sun, A. V. Fedorov, M. M. Murnane, H. C. Kapteyn, S. T. Cundiff, Y. Aiura, K. Oka, H. Eisaki, and D. S. Dessau, Phys. Rev. Lett. **96**, 017005 (2006); G. Liu, G. Wang, Y. Zhu, H. Zhang, G. Zhang, X. Wang, Y. Zhou, W. Zhang, H. Liu, L. Zhao, J. Meng, X. Dong, C. Chen, Z. Xu, and X. J. Zhou, Rev. Sci. Instrum. **79**, 023105 (2008).

[2] T. Yamasaki, K. Yamazaki, A. Ino, M. Arita, H. Namatame, M. Taniguchi, A. Fujimori, Z.-X. Shen, M. Ishikado, and S. Uchida, Phys. Rev. B **75**, 140513 (2007).

[3] E. Pedersoli, C. M. R. Greaves, W. Wan, C. Coleman-Smith, H. A. Padmore, S. Pagliara, A. Cartella, F. Lamarca, G. Ferrini, G. Galimberti, M. Montagnese, S. dal Conte, and F. Parmigiani, Appl. Phys. Lett. **93**, 183505 (2008).

[4] P. J. Feibelman, Prog. Surf. Sci. **12**, 287 (1982).

[5] J. Monin and G.-A. Boutry, Phys. Rev. B **9**, 1309 (1974); S. A. Flodstrom and J. G. Endriz, *ibid.* **12**, 1252 (1975); H. Petersen and S. B. M. Hagström, Phys. Rev. Lett. **41**, 1314 (1978); G. Jezequel, *ibid.* **45**, 1963 (1980).

[6] H. J. Levinson, E. W. Plummer, and P. J. Feibelman, Phys. Rev. Lett. **43**, 952 (1979); H. J. Levinson and E. W. Plummer, Phys. Rev. B **24**, 628 (1981).

[7] R. A. Bartynski, E. Jensen, T. Gustafsson, and E. W. Plummer, Phys. Rev. B **32**, 1921 (1985).

[8] S. R. Barman, P. Häberle, and K. Horn, Phys. Rev. B **58**, R4285 (1998).

[9] C. Schwartz and W. L. Schaich, Phys. Rev. B **30**, 1059 (1984); K.-D. Tsuei, E. W. Plummer, A. Liebsch, K. Kempa, and P. Bakshi, Phys. Rev. Lett. **64**, 44 (1990); A. Liebsch, *Electronic Excitations at Metal Surfaces* (Plenum, New York, 1997).

[10] A. J. Bennett, Phys. Rev. B **1**, 203 (1970).

[11] P. J. Feibelman, Phys. Rev. Lett. **34**, 1092 (1975); Phys. Rev. B **12**, 1319 (1975).

[12] V. U. Nazarov, Phys. Rev. B **59**, 9866 (1999).

[13] N. Barberan and J. E. Inglesfield, J. Phys. C **14**, 3114 (1981).

[14] P. Das and N. Kar, Phys. Status Solidi B **187**, 551 (1995); Z. Pachuau, B. Zoliana, D. T. Khating, P. K. Patra, and R. K. Thapa, Phys. Lett. A **275**, 459 (2000).

[15] E. E. Krasovskii, Phys. Rev. B **70**, 245322 (2004).

[16] E. E. Krasovskii and W. Schattke, Phys. Rev. Lett. **93**, 027601 (2004).

[17] *Handbook of Optical Constants of Solids*, edited by E. D. Palik (Academic, New York, 1985).

[18] D. Samuelsen and W. Schattke, Phys. Rev. B **51**, 2537 (1995).

[19] V. M. Silkin, J. M. Pitarke, E. V. Chulkov, and P. M. Echenique, Phys. Rev. B **72**, 115435 (2005).

[20] E. V. Chulkov, V. M. Silkin, and P. M. Echenique, Surf. Sci. **391**, L1217 (1997); **437**, 330 (1999).

[21] G. D. Mahan, Phys. Rev. B **2**, 4334 (1970); P. J. Feibelman and D. E. Eastman, *ibid.* **10**, 4932 (1974).

[22] E. E. Krasovskii, F. Starrost, and W. Schattke, Phys. Rev. B **59**, 10504 (1999).

[23] E. E. Krasovskii and W. Schattke, Phys. Rev. B **60**, R16251 (1999).

[24] E. E. Krasovskii and V. N. Strocov, J. Phys.: Condens. Matter **21**, 314009 (2009).

[25] E. E. Krasovskii, W. Schattke, P. Jiříček, M. Vondráček, O. V. Krasovska, V. N. Antonov, A. P. Shpak, and I. Bartoš, Phys. Rev. B **78**, 165406 (2008).